Available online at www.sciencedirect.com
SCIENCE DIRECT®
ELSEVIER
Nuclear Physics A 756 (2005) 54–82
NUCLEAR PHYSICS A

Detailed spectroscopy of ^{113}Cd through transfer reactions

D. Bucurescu [a], Y. Eisermann [b], G. Graw [b], R. Hertenberger [b], H.-F. Wirth [c,b], Yu.V. Ponomarev [d,1]

[a] *National Institute of Physics and Nuclear Engineering, Bucharest, Romania*
[b] *Sektion Physik, Ludwig Maximilians Universität München, am Coulombwall 1, 85748 Garching, Germany*
[c] *Department of Physics, E18, Technische Universität München, Germany*
[d] *Institut für Kernphysik, Technische Universität Darmstadt, D-64289 Darmstadt, Germany*

Received 27 December 2004; received in revised form 4 March 2005; accepted 15 March 2005

Available online 8 April 2005

Abstract

High energy resolution studies of ^{113}Cd have been performed with the (d, p) and (d, t) reactions, using polarized beams. In both reactions, a large number of levels (about 80) have been observed up to 2.6 MeV excitation energy, for many of them unambiguous spin and parity assignment being made. Together with previous data from other experiments, the level scheme has probably become essentially complete up to this energy. A detailed comparison is made between the experimental levels and calculations performed with the interacting boson–fermion model-1 (IBFM-1) and with the quasiparticle phonon model (QPM), which allows a good understanding of the level scheme up to about 2 MeV excitation. This nucleus is a special case for the QPM, where due to a strong anharmonicity rather complex configurations must be taken into account in order to get a good description even at low excitation energies. The multiplet structures arising from the coupling of the $3s_{1/2}$, $2d_{3/2}$, $2d_{5/2}$, and $1g_{7/2}$ neutron orbitals to the quadrupole one-phonon excitation of the core nucleus ^{112}Cd have been assigned, and the possible identification of $1/2^+$ and $3/2^+$ "intruder" states (based on two particle–two hole excitations of the core) is discussed. The observation of many $\ell = 1$ transitions above 2 MeV excitation gives a clue to the way by which the $11/2^-$ isomeric state can be populated in the (n, γ) and (γ, γ') reactions.

E-mail address: bucurescu@tandem.nipne.ro (D. Bucurescu).

[1] Permanent address: Bogoliubov Laboratory of Theoretical Physics, Joint Institute for Nuclear Research, 141980 Dubna, Russia.

0375-9474/$ – see front matter
doi:10.1016/j.nuclphysa.2005.03.012

Keywords: NUCLEAR REACTIONS ^{112}Cd($\vec{d}$, p), $E = 22$ MeV; ^{114}Cd($\vec{d}$, t), $E = 25$ MeV; measured particle spectra, $\sigma(\theta)$, Ay(θ). ^{113}Cd deduced levels, J, π, spectroscopic factors, configurations. Interacting boson–fermion model and quadrupole phonon model calculations.

1. Introduction

High resolution experiments of transfer reactions with light particles remain a very important source of detailed knowledge for the nuclear structure of the nuclei close to the valley of stability. In particular, the one-nucleon (e.g., one-neutron) transfer reactions are very sensitive probes for learning about the microscopic (single-particle) structure of the final levels. By adding such data to the information that can be deduced from other possible nuclear reactions, each one with its specific selectivity in populating the excited states, one may hope to obtain, on one hand, the complete level scheme up to a certain spin and excitation energy, and on the other hand, clear evidence for different basic excitation modes of the nuclei.

The Cadmium isotopes with neutron numbers around the middle of the 50–82 shell constituted for many years a good ground for such detailed studies. In particular, the even–even isotopes ^{112}Cd [1] and ^{114}Cd [2] have been the object of many experimental studies, which allowed to disentangle several excitation modes up to an excitation energy of about 2.6 MeV. At lower excitation energy they behave like anharmonic vibrators, exhibiting one-, two-, and three-phonon multiplets. But other excitation modes have been recognized too. For example, in ^{112}Cd, an intruder band based on a 0^+ two particle–two hole excitation state at low-energy (about 1.2 MeV) has been observed, and above 2 MeV excitation mixed-symmetry states, octupole phonon and hexadecapole phonon states have been proposed; the corroboration of different types of experiments aimed to 'read out' all this structure information is very nicely illustrated in Ref. [3].

Such a rich variety of excitations should manifest itself also in the neighboring odd-A nuclei, like the odd-A Cd isotopes. In an odd-mass Cd nucleus, since one has to couple an odd neutron which may occupy any of the five available single-particle orbitals ($3s_{1/2}$, $2d_{3/2}$, $2d_{5/2}$, $1f_{7/2}$ and $1h_{11/2}$) the resulting low-energy level scheme is rather rich; for example, by coupling these orbitals only to the quadrupole one-phonon state 2_1^+ of the even–even Cd core one expects five level multiplets with a total of 21 excited states spread over several hundreds of keV above 0.5 MeV excitation. Therefore, to study such complicated structures one needs experiments with very good energy resolution and sensitivity.

The present article presents such an experimental approach to the structure of ^{113}Cd. Apart from the nuclear structure physics, briefly sketched above, this nucleus is also of special interest for the astrophysics (nuclear synthesis in the Cd–In–Sn region). This latter aspect has been emphasized in previous papers, for example in Refs. [4,5], and resides in the fact that once formed from the β-decay of ^{113}Ag, ^{113}Cd decays either to the ground state, or to the $11/2^-$ isomer at 263 keV (half life of 14 years), which leads to the population of ^{114}Cd (by thermal neutron capture from the g.s.) and of ^{113}In (by β-decay of the isomer), respectively. The relative population of the two nuclei is also influenced by

the population of the $11/2^-$ isomer from the ground state, through the (γ, γ') reaction. The details of this process are not accurately known; the study of Ref. [4] has established some excited states populated in the (γ, γ') reaction up to 2.6 MeV excitation, many of them still requiring spin and parity assignments. As in the case of the odd-mass Tellurium isotopes with mass 123, 125, and 129 [6] it is likely that also in the case of ^{113}Cd the population of the $11/2^-$ isomeric state takes place through many negative parity low-spin states, which decay primarily through the lowest $5/2^-$ state at 855 keV, a state which 'funnels' the gamma-decay flux towards the isomeric state.

^{113}Cd is a nucleus which has been rather thoroughly studied by a wide variety of nuclear reactions [7]. As non-selective probes, are the $(n, n'\gamma)$ study [8], which evidenced a large number of levels up to about 2.3 MeV in the spin window $1/2$ to $7/2$, and the $(\alpha, n\gamma)$ reaction study [5], which mainly populated levels in a wide region above the yrast band, up to spin of about $15/2$. For many levels established in these works, especially above 1 MeV excitation, spin–parity assignments are not firm or are missing. High spin states (the $\nu h_{11/2}$ sequence) have been determined from heavy-ion fusion reaction studies [13], but these will not be discussed in the present work. Additional information comes from other probes which are more selective in populating the final levels. One of them is the beta decay [9] which populates states in the window allowed by the spin of the parent state and the selection rules. The old (p, p') [10] and (d, d') [11] reaction studies evidenced only several strongly populated levels. The (γ, γ') reaction study quoted above [4] evidenced a bunch of levels between 1.8 and 2.6 MeV excitation, most of them probably dipole excitations. Finally, a fairly large number of levels up to 2.7 MeV excitation have been assigned from the (d, p) and (d, t) reaction studies of Goldman et al. [12], many of them without firm spin–parity assignment. In this work, we present new results on excited levels in ^{113}Cd, as determined from the $(\vec{d}, p)$ reaction at 22.0 MeV, and the $(\vec{d}, t)$ reaction at 25.0 MeV, respectively. These new results extend the previous ones [12] in two directions: first, they are made with higher energy resolution, of about 5 keV FWHM, comparable with the resolution of the gamma-ray experiments; second, the use of polarized projectiles allows unambiguous spin–parity assignments. With these new improvements, we hope that the present results together with those of the previous studies lead to an almost complete determination of the level scheme up to about 2.5 MeV excitation and spin $11/2$. This allows a more detailed comparison with the predictions of different nuclear structure models, and thus a better characterization of the types of excitation met in this nucleus.

2. Experiments and results

The experiments have been performed with polarized deuterium beams delivered by the Tandem accelerator of the University and Technical University in Munich. The vector polarization P_3 of the beam, obtained with an atomic beam source [14] was around 60%. In both experiments, the reaction products were analyzed with the Munich Q3D spectrograph [15], and then detected in a 1.8 m long focal plane detector [16] which provides ΔE–$E_{\rm rest}$ particle identification and determines the position with a good resolution. For each angle two runs were measured, with spin 'up' and 'down', respectively. For each

peak in the spectrum, and at each angle, we have determined both the differential cross section σ and the analyzing power A_y

$$\sigma = \frac{\sigma^+ + \sigma^-}{2}, \qquad A_y = \frac{2}{3P_3}\frac{\sigma^+ - \sigma^-}{\sigma^+ + \sigma^-},$$

where σ^+ and σ^- are the differential cross sections measured for the two spin orientations, and P_3 is the vector polarization of the beam. The different runs were normalized to the beam current integrated into a Faraday cup placed behind the target. Some details pertinent to each experiment are specified below.

2.1. The $^{114}Cd(\vec{d},t)^{113}Cd$ reaction

The incident energy was 25.0 MeV. The target was 93 μg/cm^2 ^{114}Cd evaporated on a 17 μg/cm^2 carbon foil, and had an isotopic enrichment of 99.1%. Spectra were measured at 11 angles between 8° and 45°. The acceptance opening of the magnetic spectrograph was 9.96 msr (slit of 17 mm horizontally, 20 mm vertically). Typical current on the target was 150 nA. Fig. 1 shows an example of spectrum obtained with this reaction, at 23°. As the tritons are very well separated from other reaction products, the resulting spectra are virtually free of other contaminants. The energy resolution achieved for the spectra

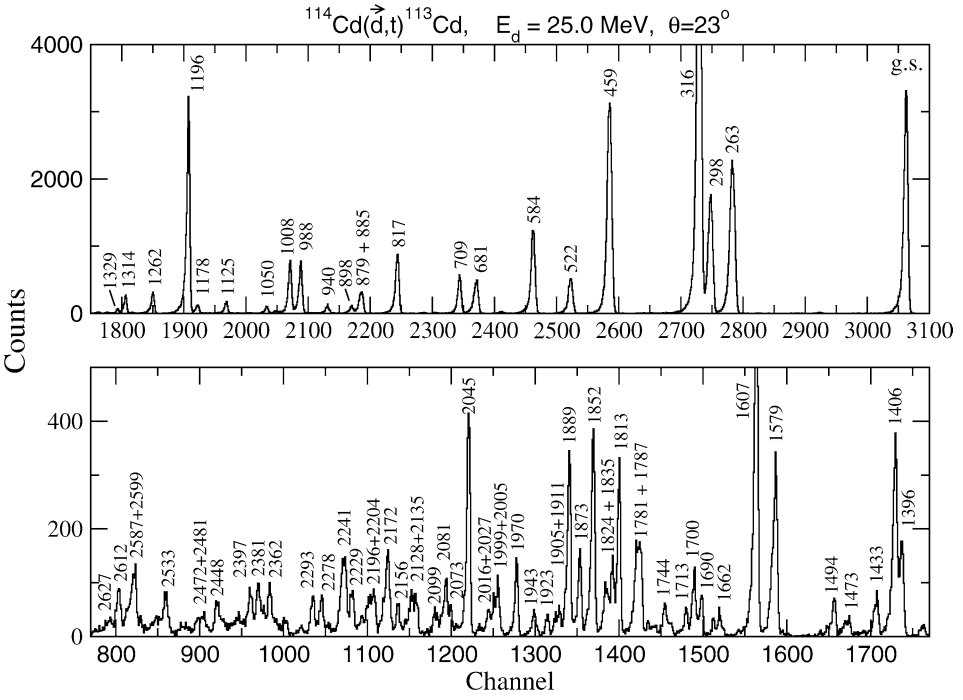

Fig. 1. Spectrum measured in the $(\vec{d},t)$ reaction at 25.0 MeV and $\theta_{\rm lab} = 23°$, for one of the beam polarizations. The peaks are labeled with their energy in keV, cf. Table 2. The spectrum was obtained in a 2 hours run, with a beam current of 150 nA.

was about 5 keV FWHM. The energy range covered by the focal plane detector for one magnetic setting of the spectrograph was about 2.7 MeV in excitation energy. Absolute energy calibration was obtained by using well-known peaks of ^{113}Cd [7]; also, at 17° the reaction ^{122}Te$(d,t)^{121}$Te [17] was measured with the same settings for the magnetic spectrograph. A third order polynomial has been used for the energy calibration function (energy versus channel number). Up to an excitation energy of 2.63 MeV we have observed 98 excited states of ^{113}Cd.

2.2. The ^{112}Cd$(\vec{d}, p)^{113}$Cd reaction

The incident energy in this case was 22.0 MeV. The target was 134 μg/cm^2 ^{112}Cd evaporated on a 17 μg/cm^2 carbon foil, and had an isotopic enrichment of 98.6%. Spectra were measured at 11 angles between 17° and 55°, with beam currents of about 100 nA. The acceptance opening of the magnetic spectrograph was 11.11 msr (slit of 20 mm horizontally, 20 mm vertically), except at small angles when it was 9.01 msr (15 mm × 20 mm). As in the case of the (d,t) reaction, the energy range up to 2.7 MeV was covered with one setting of the magnetic spectrograph. Absolute energy calibration was obtained by using well-known peaks of ^{113}Cd [7] as well as the reaction ^{144}Sm$(d,p)^{145}$Sm [18] which was measured at 40° with the same settings for the magnetic spectrograph. The achieved energy resolution was about 5 keV FWHM. A third order polynomial has been used for the energy calibration function (energy versus channel number). Fig. 2 shows a part of the spectrum recorded at 35°; in this case it is compared with a spectrum measured at 50° with the reaction $(\alpha, {}^3\mathrm{He})$ at an incident energy of 33.0 MeV. The latter spectrum has been measured with a target 143 μg/cm^3 thick on 17 μg/cm^3 Carbon foil, and has an energy resolution of 50 keV FWHM. Up to 1.7 MeV excitation (the range seen in the latter case) the two one neutron stripping reactions show the excitation of similar peaks. However, the different conditions of angular momentum matching make that the $(\alpha, {}^3\mathrm{He})$ favors the population of the states of higher spin (see the discussion below). Up to an excitation energy of 2.63 MeV we have observed 75 excited states of ^{113}Cd with the (d,p) reaction.

2.3. DWBA analysis and results

In order to determine the values of the transferred angular momentum (ℓ) and spin (j) for each level, therefore to deduce its spin J and parity, we have compared the experimental angular distributions with predictions of DWBA calculations. These calculations have been performed with the code CHUCK3 [19]. The optical model parameters for the entrance and exit channel, respectively, have been chosen according to the existing compilations [20], and are specified in Table 1 for both reactions. The (d,p) reaction measures the degree of emptiness of a neutron shell model orbital, therefore in this case the expected (ℓ, j) transfers in the low excitation energy correspond to the orbitals from the 50–82 shell ($3s_{1/2}$, $2d_{3/2}$, $2d_{5/2}$, $1g_{7/2}$, $1h_{11/2}$), and small fragments of the orbitals from the higher shell ($3p_{1/2}$, $3p_{3/2}$, $2f_{5/2}$, $2f_{7/2}$). The (d,t) reaction measures the degrees of fullness, therefore the observed transfer should correspond to the same orbitals, and eventually to the distant orbitals from the shell below ($1g_{9/2}$, $2p_{1/2}$, $2p_{3/2}$, $1f_{5/2}$, $1f_{7/2}$). By normalizing the calculated cross section to the experimental one, one gets the spectroscopic factors

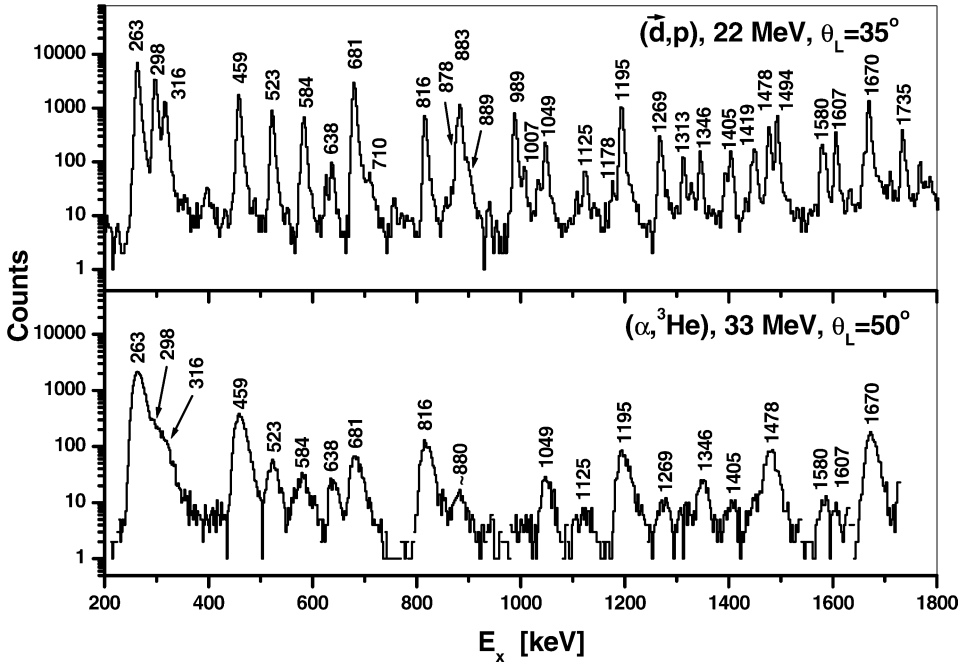

Fig. 2. Portion of the spectrum measured in the $(\vec{d}, p)$ reaction at 22.0 MeV and $\theta_{\rm lab} = 35°$, for one of the beam polarizations. The spectrum was obtained in a two hours run, with a beam current of 60 nA. This spectrum is compared to one of the $(\alpha, {}^3{\rm He})$ reaction measured at 33 MeV and $\theta_{\rm lab} = 50°$; no angular distributions have been measured in the latter case.

Table 1
Optical model parameters [20] used in the DWBA calculations

	^{114}Cd(d,t), 25.0 MeV			^{112}Cd(d,p), 22.0 MeV		
	d	t	n	d	p	n
V_r	96.5	150.24	Adj.	114.28	56.15	Adj.
$4W_D$	48.0	20.0		70.0	18.26	
W_0					3.09	
V_{so}	7.40		$\lambda = 25$	13.71	13.71	$\lambda = 25$
r_r	1.133	1.24	1.17	1.143	1.12	1.17
r_D	1.325	1.43		1.32	1.122	
r_0					1.122	
r_{so}	1.07			1.07	1.01	
r_C	1.15	1.25		1.15	1.25	
a_r	0.77	0.687	0.75	0.77	0.75	0.75
a_D	0.68	0.87		0.748	0.61	
a_0					0.61	
a_{so}	0.66			0.66	0.75	
Non-loc.	0.54	0.25	0.85	0.54	0.85	0.85

S_{lj} or the spectroscopic strength G_{lj} in the following way: $\sigma_{\rm exp} = S_{lj}\sigma_{lj}^{\rm Chuck}$ for the (d, p) reaction, and $\sigma_{\rm exp} = G_{lj}\sigma_{lj}^{\rm Chuck}$ for the (d, t) reaction, respectively, with $G_{lj} = (2j+1)S_{lj}$.

Fig. 3 shows examples of DWBA analysis for each of the observed (ℓ, j) transfers, and both reactions. One should note the sensitivity of the analyzing power to the value of the total transferred spin j, which leads to the unambiguous determination of the final level spin value $(J = j)$. For most of the levels, one could determine a unique ℓ value, as expected for a direct transfer reaction mechanism. The distinction between the two possible values $j = \ell + 1/2$ and $j = \ell - 1/2$ could be made for many of the populated levels, on the basis of the analyzing power. There are, however, some levels for which this distinction was not possible due to insufficient statistical level of the data. In general, the data from the (d, t) reaction have more structured angular distributions, which allow more clear (ℓ, j) assignments. There are also levels which have been observed only in one of the two reactions. In addition, a small number of levels did not show an angular distribution characteristic to a given ℓ-value; this may indicate that they are populated by multi-step processes (which is clearly the case of the $13/2^-$ level at 1109 keV) or, in several cases it is due to unresolved doublets. Some systematic deviations of the experimental data from the predicted DWBA patterns, especially in the case of the asymmetry, may indicate, even in the case of some low-lying levels, coupled channel effects (multi-step excitation mechanisms); in such cases, the quoted spectroscopic factor values represent just an upper limit.

The whole information obtained from the two reactions is contained in Table 2, where the adopted levels of Ref. [7], based on all previous experiments, are also listed. There is a good correspondence between the excitation energies of the levels observed in the present work with the two reactions, and in most of the cases one can find correspondences with levels observed before, for many of these a better J^π assignment being possible. One should note that we have included in the NNDC columns ('adopted levels') all the levels determined from the (γ, γ') experiment of Ref. [4] (marked with 'd' in the table), which, with the exception of the 2588 keV one, have been observed at least in one of our reactions. Different comments on the excited states will be made below on the occasion of the comparison with theoretical model calculations. Here we highlight just a few of the achievements of the present work, which bring a better knowledge of the low-energy level scheme of ^{113}Cd. We confirm the spin–parity $1/2^+$ proposed in Ref. [8] for the 1050 keV level and assign other new $1/2^+$ levels (e.g., those at 2080 and 2135 keV). The first (and only) $1/2^-$ level known in this nucleus was unambiguously identified at 2044 keV; it corresponds to the 2044 keV state observed in the (γ, γ') experiment and assigned as $(3/2^-, 1/2^-)$ [4]. Unambiguous $3/2^+$ assignments are made to the levels at 879, 1302, 1493 keV, while the levels at 1008, 1178, 1195, 1366, 1406 keV are assigned as $5/2^+$, and those at 1261 and 1433 keV as $7/2^+$, respectively. We find a significant fraction of the $h_{11/2}$ orbital ($11/2^-$ levels), populated, as expected, especially in the (d, p) reaction. Both in the (d, p) and the (d, t) reaction we find several $7/2^-$ states which hint to the importance of the $2f_{7/2}$ orbital in the structure of the low-lying states. Then, at higher excitation energy we find a large number of $\ell = 1$ states; some of them correspond to the levels observed in the (γ, γ') reaction where one expects to excite dipole modes [4].

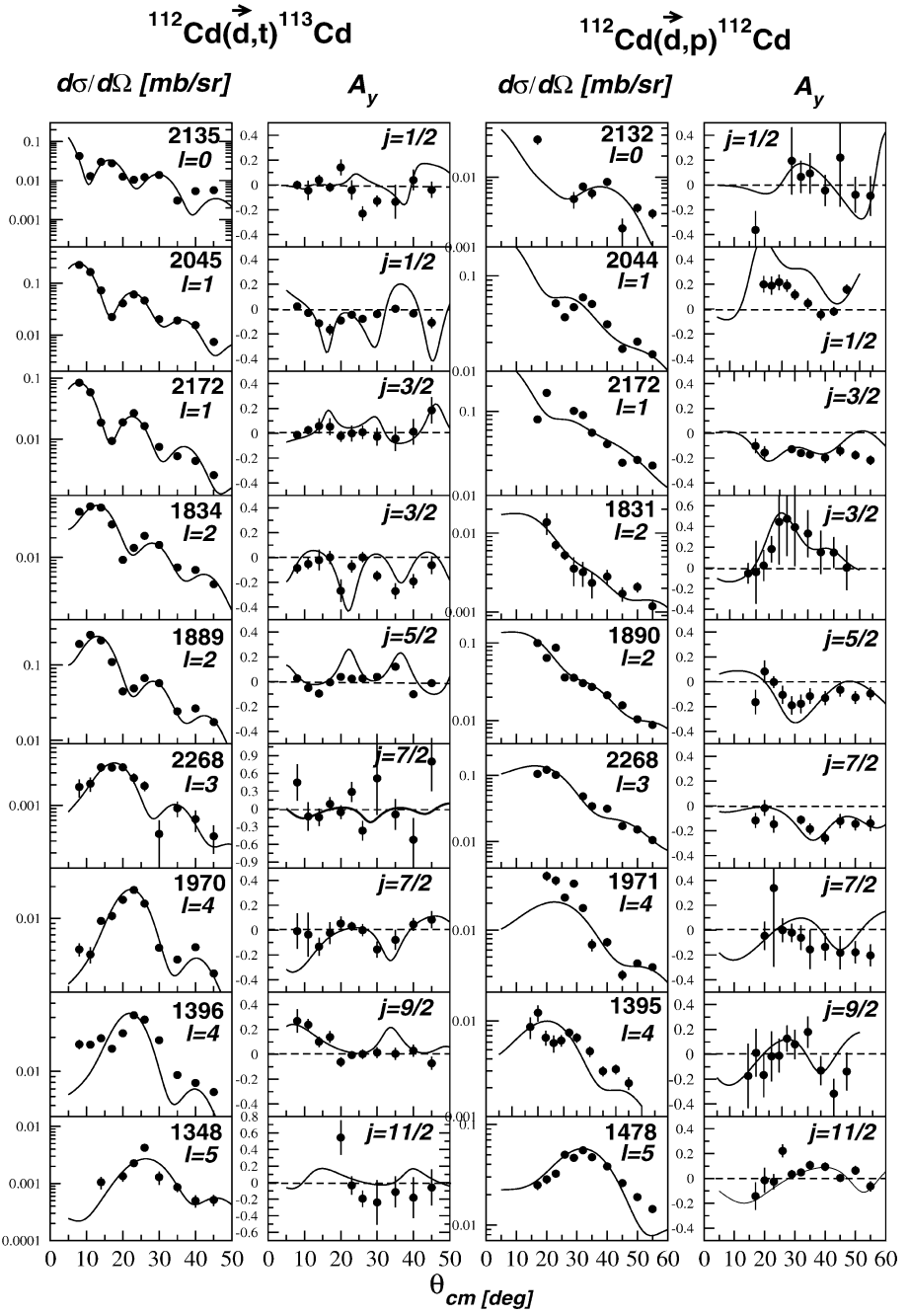

Fig. 3. Examples of angular distributions and assymetries measured with the present two experiments. The continuous curves are predictions of the DWBA calculations described in the text. The labels indicate the energy of the level as measured in each reaction (Table 2), and the assigned (ℓ, j) transfer.

Table 2
List of ^{113}Cd level energies and spectroscopic factors, as observed in the present study with the $(\vec{d}, t)$ and $(\vec{d}, p)$ reactions, compared to previously known levels [7]

$(\vec{d}, t)$ (present)					NNDC [7]		$(\vec{d}, p)$ (present)				
E_x[a]	ℓ	J^π	σ[c]	$10G_{lj}$	E_x	J^π	E_x[b]	ℓ	J^π	σ[c]	$10S_{lj}$
0	0	$1/2^+$	3135	2.45	0	$1/2^+$	0	0	$1/2^+$	703	2.53
262.5	5	$11/2^-$	563	9.46	263.54(3)	$11/2^-$	263.9	5	$11/2^-$	1069	4.30
297.7	2	$3/2^+$	2304	2.51	298.597(10)	$3/2^+$	298.3	2	$3/2^+$	1994	2.37
315.5	2	$5/2^+$	6153	6.18	316.206(15)	$5/2^+$	316.3	2	$5/2^+$	875	0.67
458.6	4	$7/2^+$	783	11.96	458.633(17)	$7/2^+$	458.7	4	$7/2^+$	376	1.92
522.3	3	$7/2^-$	314	1.36	522.259(24)	$7/2^-$	522.6	3	$7/2^-$	416	0.30
					530(10)	$7/2^+,\ 9/2^+$					
584.8	2	$5/2^+$	1090	1.01	583.962(24)	$5/2^+$	583.8	2	$5/2^+$	345	0.29
							626.6	2	$(3/2^+)$	23	0.020
638.2	(5)	$(9/2^-)$	5	0.15	638.19(3)	$9/2^-$	637.8	5	$9/2^-$	12	0.11
681.5	2	$3/2^+$	748	0.77	680.526(20)	$3/2^+$	680.6	2	$3/2^+$	1228	1.48
709.5	2	$5/2^+$	346	0.33	708.571(19)	$5/2^+$	709.5	2	$5/2^+$	23	0.019
					760(10)	$1/2^+$					
					815.34(3)	$15/2^-$					
817.4	4	$7/2^+$	195	2.98	816.707(22)	$7/2^+$	816.4	4	$7/2^+$	124	0.58
					855.28(3)	$5/2^-$					
					869.81(22)	$15/2^-$					
879.8	2	$3/2^+$	374	0.38	878.54(6)	$(3/2^+)$	877.7	(2)	$(3/2^+)$	64	~ 0.078
884.8	0	$1/2^+$	98	0.063	883.62(6)	$1/2^+$	883.3	0	$1/2^+$	190	0.55
898.4	(2)	$(3/2^+)$	19	0.031	897.53(4)	$3/2^+$	899.1	(2)		14	~ 0.027
940.4	4	$9/2^+$	21	0.20	939.788(19)	$9/2^+$	939.5			2	
					960(10)						
989.0	0	$1/2^+$	665	0.28	988.40(6)	$1/2^+$	989.1	0	$1/2^+$	93	0.32
					999.42(7)						
					1002.87(4)	$3/2^+$					
1008.2	2	$5/2^+$	534	0.41	1007.20(5)	$(5/2^+)$	1007.1	2	$5/2^+$	33	0.026
1033.5	2	$(3/2^+)$	187	0.015	1034.09(6)	$(3/2^+)$	1035.9	2	$(3/2^+)$	20	0.025
					1037.40(3)	$(5/2, 7/2^+)$					
					1047.65(4)	$7/2^+$					
					1049.66(9)	$3/2^+$					
1050.7	0	$1/2^+$	67	0.033			1048.9	(0)	$(1/2^+)$	43	~ 0.11
					1051.248(22)	$7/2^-$					
1108.4			1		1109.32(3)	$13/2^-$	1108.9			1	
					1124.636(20)	$9/2^+$					
1125.9	2	$(3/2^+)$	14	0.04			1124.9	(4)		8	~ 0.017
					1126.25(6)	$3/2^+$					
					1170(20)						
					1177.722(23)	$(9/2^-)$					
1178.3	2	$5/2^+$	114	0.077	1177.8(3)	$(3/2^+)$	1178.1	2	$5/2^+$	14	0.0087
					1181.35(4)						
					1190.72(5)						
					1192.09(4)						
					1194.6(2)	$3/2^-$					
1196.1	2	$5/2^+$	2560	1.75	1195.30(20)	$5/2,\ 7/2^+$	1194.6	2	$5/2^+$	401	0.33
					1209.53(15)	$13/2^-$					
					1214.674(22)	$11/2^+$					

Table 2 (*continued*)

$(\vec{d},t)$ (present)					NNDC [7]		$(\vec{d},p)$ (present)				
E_x[a]	ℓ	J^π	σ[c]	$10G_{lj}$	E_x	J^π	E_x[b]	ℓ	J^π	σ[c]	$10S_{lj}$
1262.5	4	$7/2^+$	59	0.72	1261.92(4)	(9/2)					
					1268.21(5)	$3/2^+$	1269.1	2	$3/2^+$	142	0.13
					1279.62(7)	$3/2^+$					
1302.2	2	$3/2^+$	16	0.014	1301.07(7)	$3/2^+$, $5/2^+$					
							1312.9	(5)	$(11/2^-)$	12	0.047
1314.4	(4)	$(9/2^+)$	26	0.36	1313.75(3)	$(5/2^+)$					
					1322.02(12)	$(7/2^-, 9/2^-)$					
					1327.6(4)						
1329.8	4	$7/2^+$	8	0.12			1329.4	(4)	$(7/2^+)$	4	0.013
1348.3	5	$11/2^-$	4	0.044	1346.53(4)	$11/2^-$	1346.4	5	$11/2^-$	18	0.068
					1351.58(7)	5/2, 7/2					
1366.2	2	$5/2^+$	9	0.0067	1364.76(7)	$(5/2^+)$					
					1367.569(24)	$7/2^+$					
					1387.47(8)	$5/2^+$, $3/2^+$					
					1390.56(9)	$(1/2^+, 3/2^+)$					
1396.5	4	$9/2^+$	31	0.26	1395.83(3)	$(9/2^+)$	1394.8	(4)	$(9/2^+)$	12	0.019
1406.0	2	$5/2^+$	262	0.18	1405.82(10)	$(1/2^+, 3/2^+)$	1404.6	2	$5/2^+$	55	0.043
					1407.5(3)	$(9/2^+)$					
					1410.68(6)						
					1430(10)	$(3/2^+)$					
1433.0	4	$7/2^+$	14	0.18							
1452.3			2		1450.30(7)		1449.2	5	$11/2^-$	32	0.10
					1461.67(4)						
1473.4			10								
							1477.9	5	$11/2^-$	55	0.19
					1479.08(5)	$3/2^+$					
1493.9	2	$3/2^+$	80	0.057	1493.03(9)	$1/2^+$, $3/2^+$	1493.7	2	$3/2^+$	215	0.23
					1504.90(4)	$7/2^+$					
					1513.72(4)						
					1542.28(9)	$(1/2^+)$					
					1561.69(3)	+					
					1575.66(14)	$7/2^-$					
1579.2	2	$(5/2^+)$	267	0.164			1580.0	2	$(3/2^+)$	115	0.23
1607.6	2	$5/2^+$	571	0.36	1607.21(10)	$5/2^+$	1606.9	2	$5/2^+$	109	0.081
					1620.43(3)						
					1626.41(4)						
					1647.23(5)						
					1657.41(5)	$11/2^-$					
					1658.51(7)						
1662.2	(2)	$(3/2^+)$	69	0.033			1661.2	2	$3/2^+$	28	0.034
					1670.89(10)		1670.4	5	$(11/2^-)$	154	0.48
					1675.09(9)	$3/2^+$					
1689.6			39								
1700.1	(5)	$(11/2^-)$	18	0.34							
							1711.0	(2)		10	0.009
1713.0	(1)	$(3/2^-)$	35	0.010							
					1732.84(4)	$11/2^+$					
							1735.0	5	$11/2^-$	42	0.128
					1737.53(7)						

(*continued on next page*)

Table 2 (*continued*)

$(\vec{d},t)$ (present)					NNDC [7]		$(\vec{d},p)$ (present)				
E_x[a]	ℓ	J^π	σ[c]	$10G_{lj}$	E_x	J^π	E_x[b]	ℓ	J^π	σ[c]	$10S_{lj}$
1744.1	2	$(5/2^+)$	66	0.032	1743.56(21)						
					1746.00(14)	$(3/2^-)$					
					1758(10)	$(5/2^-,\ 7/2^-)$					
1769.4	2	$(3/2^+)$	13	0.010			1769.1	2	$(3/2^+)$	21	0.033
					1778.92(10)	$9/2^-$					
1781.4	2	$(3/2^+)$	95	0.088							
1786.5	2	$(3/2^+)$	66	0.079							
							1788.9	(0)	$(1/2^+)$	3	0.016
					1798.89(12)	$(1/2, 3/2)$					
1813.1	4	$(7/2^+)$	46	0.54							
					1813(10)	$(1/2, 3/2)$	1814.5	(2)		53	0.028
					1823.24(4)	$13/2^-$					
1825.1	2	$5/2^+$	90	0.057							
1833.5	2	$3/2^+$	61	0.050			1830.8	2	$3/2^+$	96	0.012
					1842.74(13)	$(3/2^-)$					
1852.3	0	$1/2^+$	243	0.094			1848.6	(0)	$(1/2^+)$	8	0.023
					1867.86(8)	$7/2^-,\ 9/2^-$					
1873.4	2	$3/2^+$	164	0.13	1871.7(3)						
1889.0	2	$5/2^+$	250	0.154			1890.1	2	$5/2^+$	99	0.053
					1892.32(11)	$7/2^-$					
					1896.44(4)						
					1900(10)	$(1/2^+)$					
					1902.41(5)	$13/2^-$					
					1903.97(9)						
1905.0	(3)	$(7/2^-)$	12	0.042	1904.35(11)	$(5/2, 7/2)$	1906.9	3	$7/2^-$	208	0.089
1911.4	(2)	$(5/2^+)$	11	0.011							
1923.3	2	$5/2^+$	25	0.016							
1943.0	2	$(3/2^+)$	32	0.026	1942		1940.2			20	
1969.8	4	$7/2^+$	18	0.22			1970.8	(4)		23	0.034
					1986(10)	$5/2^-,\ 7/2^-$					
1998.8	(5)	$(11/2^-)$	15	0.28			1999.7			34	
2005.3			7								
2015.6	0	$1/2^+$	22	0.007							
2027.7			2								
					2042.06(6)						
2044.9	1	$1/2^-$	225	0.089	2044[d]	$(3/2^-, 1/2^-)$	2044.1	1	$1/2^-$	59	0.14
					2046.23(7)	$15/2^+$					
2062.9			2								
2072.7	2	$5/2^+$	38	0.056							
2080.9	0	$1/2^+$	64	0.023	2080(10)	$(1/2^+)$	2080.4	(0)	$(1/2^+)$	15	0.029
2099.2	2	$5/2^+$	28	0.017							
					2113.04(22)	$7/2^-$	2110.2	(3)	$(7/2^-)$	11	0.0044
					2120(20)						
2127.6			9								
2135.0	0	$1/2^+$	42	0.013	2140(20)	$(1/2^+)$	2132.1	(0)	$(1/2^+)$	2	0.025
2145.1	(3)	$(7/2^-)$	5	0.0058	2146.81(5)		2144.9	(2)		134	0.08
2155.7	2	$3/2^+$	46	0.032							
					2164.48(11)						

Table 2 (*continued*)

$(\vec{d},t)$ (present)					NNDC [7]		$(\vec{d},p)$ (present)				
E_x[a]	ℓ	J^π	σ[c]	$10G_{lj}$	E_x	J^π	E_x[b]	ℓ	J^π	σ[c]	$10S_{lj}$
2172.2	1	$3/2^-$	83	0.028	2173.60(12)	$3/2^-$	2172.4	(1)	$(3/2^-)$	166	0.098
2179.9	2	$5/2^+$	31	0.017							
					2180(10)	$(3/2^-)$					
2195.6	1	$1/2^-$, $3/2^-$	43	0.019			2195.8	(1)	$(3/2^-)$	71	0.037
2203.5	4	$7/2^+$	9	0.10							
2213.8	(3)	$(7/2^-)$	5	0.020			2214.6	3	$7/2^-$	112	0.045
					2219.64(4)						
2229.0	(2)	$(3/2^+)$	49	0.028							
2241.1	2	$5/2^+$	115	0.062							
					2240(10)	$(5/2^-, 7/2^-)$	2242.1	(3)	$(7/2^-)$	251	0.095
							2252.9	(3)		93	0.063
2267.6	3	$5/2^-$, $7/2^-$	4	0.019	2270(10)		2268.2	3	$7/2^-$	122	0.054
2278.3	0	$1/2^+$	49	0.014							
							2288.7			34	
2292.9	4	$7/2^+$	12	0.159							
2313.5	(2)		12								
					2319.62(18)	$3/2^-$	2316.9	(1)	$(3/2^-)$	36	0.034
					2330(10)		2327.4	(1)	$(3/2^-)$	23	0.014
2336.4			13		2335[d]						
2352.0	2	$3/2^+$	16	0.012	2354[d]		2349.2			11	
2361.9	2	$5/2^+$	13	0.045			2365.2			22	
2381.1	1	$(3/2^-)$	48	0.020			2380.0	(1)	$(3/2^-)$	31	0.029
2396.6	2	$5/2^+$	91	0.049							
2413.3	2	$(3/2^+)$	37	0.024	2410(10)		2409.0	(2)		69	0.047
2425.1			5		2428[d]	$3/2^-$, $1/2^-$	2424.1	(1)	$(3/2^-)$	273	0.13
2438.9	2	$(3/2^+)$	27	0.017	2440(10)						
2448.4	2	$3/2^+$, $5/2^+$	39	0.027	2449[d]		2450.6	(1,2)		103	
2472.3	2	$3/2^+$, $5/2^+$	27	0.017							
2480.8			14				2477.2	(1)	$(3/2^-)$	56	0.046
							2487.9	(1)	$(3/2^-)$	19	0.027
2499.6	0	$1/2^+$	15	0.0029			2500.4			8	
2533.7	(2)		44	0.022	2535[d]	(3/2)					
					2540(10)	$(7/2^-)$	2537.9	(3)		25	0.012
2548.3	2	$3/2^+$, $5/2^+$	26	0.015	2545[d]						
					2556[d]		2555.9	1	$3/2^-$	56	0.046
2575.4			17		2580(10)	$(3/2^-)$					
2586.6	0	$1/2^+$	94	0.024							
					2588[d]	$3/2^-$					
							2591.7	(1)	$(3/2^-)$	41	0.004
2599.1	2	$(5/2^+)$	34	0.017							
2612.2	2	$3/2^+$, $5/2^+$	69	0.039							
2627.1	0	$1/2^+$	19	0.0041	2630(10)	$(1/2^+)$					
							2632.7	2	$(5/2^+)$	245	0.11

[a] Energy level accuracies are ±1.4 keV up to about 2.0 MeV excitation (generally lower up to $E_x = 1.5$ MeV), and ±2.5 keV afterwards;

[b] Energy level accuracies are ±1.2 keV up to about 2.1 MeV excitation (generally lower up to $E_x = 1.5$ MeV), and ±2.5 keV afterwards;

[c] Maximum differential cross section in μb/sr;

[d] Level observed in the (γ,γ') reaction (Ref. [4]).

3. Comparison with model calculations

3.1. The interacting boson–fermion model

A first comparison of the experimental information on the low-energy structure of ^{113}Cd is made with results of calculations with the interacting boson–fermion model (IBFM). We use the variant of this model which does not distinguish between the neutron and proton bosons (IBFM-1) [21]. The calculations are similar to those of Ref. [5], with some differences, however, which will be described below. The Hamiltonian of the model and the procedure for choosing the model parameters are similar to those used in the description of the odd mass Tellurium isotopes (see, for example, Ref. [17]). ^{113}Cd is described as one neutron coupled to the core nucleus ^{112}Cd, which is described by the IBM-1 (interacting boson model-1) [22] (the variant with only s and d bosons).

3.1.1. The ^{112}Cd core

First we discuss the parameterization of the core nucleus. As emphasized in the introduction, ^{112}Cd is a rather well studied nucleus, in which a multitude of excitation modes have been recognized, and the IBM-1 is not able to describe all of them. One has therefore to point out the limitations of this description from the beginning, and thus be aware of the limitations expected for the description of ^{113}Cd. Fig. 4 shows a comparison of our IBM-1

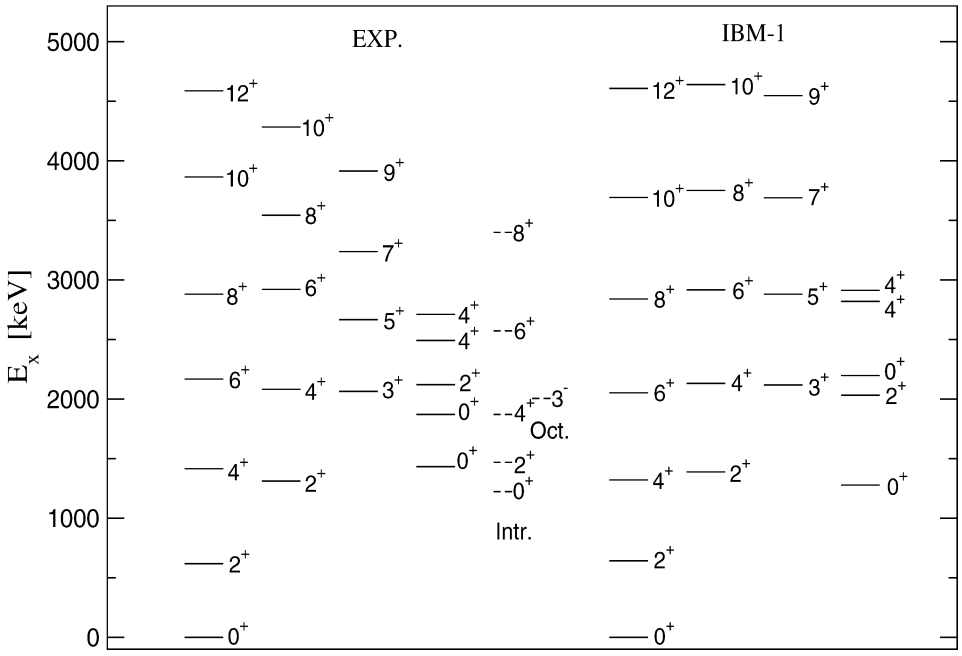

Fig. 4. The IBM-1 description of the core nucleus ^{112}Cd. The low-spin experimental levels are shown only up to about 3.0 MeV. The experimental intruder band (introduction) and the octupole phonon vibration 3^- states (October), which are out of the space of the IBM-1 model, are also drawn; see the discussion in the text, Section 3.1.

description of ^{112}Cd with a selection of experimental levels (up to about 2.7 MeV excitation, all known experimental levels are shown). Our calculations were made with the codes PHINT (energy levels) and FBEM (for the electromagnetic transition rates) [23], by numerically diagonalizing the Hamiltonian written in the usual non-multipole form [22,23]. In the notations of PHINT, the parameters used are HBAR $= 0.68$, $F = 0.08$, $G = -0.03$, $c_L(L = 0, 2, 4) = 0.030$, 0.010, 0.040, all in MeV. For the electromagnetic transition operators, as in the case of the Te isotopes [17], we have used the following: a quadrupole operator proportional with the one of the equivalent multipole form of the Hamiltonian (for the E2 transitions), and a second-order operator as defined in Ref. [24] for the M1 transitions, such as to be able to describe E2, M1, and E2/M1 mixing ratios. The exact parameters are given in [17], here we specify only the parameters entering the input to the code FBEM: EFF $= 0.10$ (boson effective charge), E2SD $= 1.0$, E2DD $= -2.98$, M1 $= 0.035$, M1E2 $= 1.0$, M1ND $= 0.0$. With these parameters for the Hamiltonian and transition operators, we were able to describe well excitation energies, transition probabilities, known branching ratios and mixing ratios for the lowest states (2_1^+, 2_2^+, 2_4^+, 3_1^+, 4_2^+, 4_3^+, and the two 0^+ states at 1433 and 1871 keV). The spectrum is rather close to that of an oscillator with some anharmonicity (the $U(5)$ dynamical symmetry of IBM-1), up to 2.5 MeV one can observe easily the members of the two- and three-phonon multiplets, as remarked in many publications before (e.g., [3,5,25,26]). However, there are experimental states which represent excitation modes which are not incorporated in the sd IBM-1 model. Fig. 4 shows only the lowest such modes. First, there is the so-called intruder band, based on a low two particle–two hole 0^+ state at 1305 keV, and then is the octupole phonon vibration—the 3^- state. In our IBM description of the core we do not include f-bosons, therefore the 3^- state cannot be described. The intruder states are also not contained in our model. By coupling one neutron either to the octupole state 3^-, or to the intruder states, one can get states in ^{113}Cd which will not be described by the IBFM-1 model. Such states, outside of our model space, are expected above 1 MeV excitation energy, and it is a challenge to recognize them. Both the 'normal' and 'intruder' states of ^{112}Cd have been well described by mixing two boson configurations: the 'normal' N-boson one, and the 'intruder', more deformed configuration, with $N + 2$ bosons ([25] and references therein). The interesting result is that the influence of the intruder states is not too strong, and it has a local character, i.e., only some levels can be strongly mixed (for example, the intruder 0^+ with the second 0^+ level). Thus, with our IBFM-1 description one can hope to be able to describe the low-energy level scheme, where should be the multiplets expected by coupling the different active shells to the quadrupole one-phonon state of the core.

3.1.2. The odd-A nucleus

In addition to an IBM-1 description of the core nucleus, the calculation for the odd-A nucleus requires a choice of the several other ingredients and parameters entering the Hamiltonian of the IBFM-1. For many of these, we have started from the values of the IBFM-1 calculations of Warr et al. [5]. The calculations have been performed with the codes ODDA (energy levels), PBEM (electromagnetic transition rates), and SPEC (one-nucleon transfer spectroscopic factors) [27]. The Hamiltonian contains, in addition to the IBM-1 term, a single quasiparticle energy term, and a boson–fermion interaction term [21]. The quasiparticle energies and shell occupancies were generated by a BCS calculation with

a pairing gap of 1.5 MeV, starting from a set of single particle energies given in Ref. [5] for the $3s_{1/2}$, $2d_{3/2}$, $2d_{5/2}$, $1g_{7/2}$, $1h_{11/2}$ orbitals, which slightly modified that of Ref. [28]. The quasiparticle energies and shell occupancies used for the positive parity orbitals and for the $1h_{11/2}$ orbital are those of Ref. [5]. For the positive parity case, the odd neutron was allowed to occupy the four orbitals of above. In the negative parity case, we have tried two separate calculations, one in which we have added to the $h_{11/2}$ orbital the orbitals from the upper major shell ($2f_{7/2}$, $1h_{9/2}$, $3p_{3/2}$ and $3p_{1/2}$), and one in which the ($1f_{7/2}$, $1f_{5/2}$, $2p_{3/2}$ and $2p_{1/2}$) of the lower major shell were considered. Actually, since we add a *particle*-type fermion to the core, the first choice is the natural one. The fact that we see in both reactions some $f_{7/2}$ strength but not at all $f_{5/2}$ strength indicates the importance of the upper major shell. In each case of the negative parity calculations, the relative single particle energies of the distant orbitals have been taken equal to those calculated with the universal Woods–Saxon potential of Ref. [29]. Relatively to the $2d_{5/2}$ shell, these values were (in MeV): 7.08 ($f_{7/2}$), 8.52 ($p_{3/2}$), 9.45 ($p_{1/2}$), 9.70 ($h_{9/2}$); we have slightly adjusted only the value for the $f_{7/2}$ orbital to 6.50 MeV (see below). The quasiparticle energies and shell occupancies (ε_j/v_j^2) used for the distant orbitals, are: $2f_{7/2}$: 5.37/0.020; $3p_{3/2}$: 7.34/0.0105; $3p_{1/2}$: 8.24/0.0083; $1h_{9/2}$: 8.49/0.0078.

Once the quasiparticle energies and shell occupancies have been obtained by these BCS calculations, one has to define the parameters of the boson–fermion interaction. This interaction has three terms [21]: a monopole–monopole, a quadrupole–quadrupole, and an exchange interaction. For these terms, the code ODDA employs the usual semi-microscopic parameterization of Ref. [30], and therefore the full boson–fermion interaction is specified by three strength parameters, which in the code are named A_0, Γ_0, and Λ_0, respectively. For these parameters we have started with the values given in Ref. [5], but, looking for a better description of the level scheme, we have finally used the following values: $A_0 = -0.10$ MeV, $\Gamma_0 = 0.20$ MeV, and $\Lambda_0 = 0.95$ MeV^2. We have also used a value of $\chi = -2.98$ for the constant used in the definition of the boson quadrupole operator, identical to the one used in the core (which differs from the value -0.1 used in [5]); the need of large χ-values for transitional and even vibrational nuclei has recently been emphasized in Ref. [31]. Both calculations, for the positive and negative parity, have been performed with the same values of the Hamiltonian parameters, and the calculations yield also a correct excitation energy for the lowest $11/2^-$ state relatively to the lowest $1/2^+$ state: 273 keV, compared to the experimental value of 264 keV. For the electromagnetic transition operators we took the same form as in the case of the core, the odd particle contribution being considered through the effective gyromagnetic factors $g_l = 0$ and $g_s = -2.6789\mu_N$ (0.7 of the free value). The calculation of the spectroscopic factors for the stripping and pickup of one neutron requires only the wave functions of the ground state of the nuclei ^{112}Cd and ^{114}Cd (calculated with IBM parameters similar to those of ^{112}Cd), and of the final level in ^{113}Cd, and no additional parameters; the transfer operators used by the program SPEC are those defined in Ref. [32].

3.2. The quasiparticle phonon model

The quasiparticle phonon model (QPM) has been successfully applied to both even-even nuclei [33] and to odd mass nuclei (see, e.g., [34–38]). As in the IBM calculations

in the previous subsection, the ground and excited states of odd-mass nuclei are described in the QPM by wave functions which include configurations made up from an unpaired quasiparticle coupled to phonon excitations of the even–even core. A distinctive feature of the QPM calculation in comparison with the IBM, is that the structure of phonons is obtained microscopically by solving the quasiparticle RPA equations. First of all, we solve the BCS equations, separately for neutrons and protons. We use the Woods–Saxon potential for the mean-field with parameter sets from Ref. [39] for neutrons and from Ref. [40] for protons. The monopole pairing strength parameter is adjusted to reproduce experimental values for the pairing energies in neighboring nuclei. For ^{112}Cd, the used values are 0.134 and 0.182 MeV for neutrons and protons, respectively. As a result, we obtain the quasiparticle spectrum and particle–hole occupation numbers u_j^2 and v_j^2. Next, we build phonons from neutron and proton quasiparticle pairs. Phonon energies and the internal fermion structure of phonons is obtained by solving the quasiparticle RPA equations. For ^{112}Cd core, we have calculated the spectrum of natural parity phonons with the multipolarity from 0^+ to 7^- except for 1^- phonons which do not contribute at low excitation energies. The strength parameters of the residual interaction have been adjusted to the experimental B(E2) and B(E3) values of the lowest 2_1^+ and 3_1^- states in ^{112}Cd. We have used the separable form of the residual interaction with the form-factor as a derivative of the mean field. The isoscalar strength of the residual interaction equals to 0.0145 fm^2/MeV for positive parity phonons and 0.0165 fm^2/MeV for negative parity phonons. The spectrum of phonons includes both collective phonons and practically pure two-quasiparticle states. In other words, besides the lowest, most important, collective phonons like 2_1^+, 3_1^-, 4_1^+, other less collective phonons are considered. Finally, we perform diagonalization of the QPM Hamiltonian on a set of wave functions which include quasiparticle (qp) and quasiparticle–n-phonon configurations (qp $\otimes$ $n$ph) in the odd ^{113}Cd nucleus for different values of the total angular momentum j^π from $1/2^\pm$ to $11/2^\pm$ and for $j^\pi = 13/2^-$ and $15/2^-$. In the present calculations $n = 1, 2, 3$. This diagonalization yields excitation spectrum of ^{113}Cd and wave functions of all excited states. Since the excitation energy of the 2_1^+ state in ^{112}Cd is very low and anharmonic effects are rather strong in this nucleus, inclusion of the qp $\otimes$ 3ph configurations in the model space is rather important even at excitation energies below 2 MeV. We refer to Refs. [34,41,42] for more detailed description of the QPM calculations in odd-mass nuclei.

Accounting for the interaction between different components of the wave function leads to renormalization of the excitation energy from its harmonic limit. The shift ΔE_n which an $n$ph (or qp$\otimes n$ph) configuration receives due to its interaction with an n'ph configuration can be estimated perturbatively as

$$\Delta E_n \approx \frac{[V_{n'}^n]^2}{E_n - E_{n'}}, \tag{1}$$

where $V_{n'}^n$ is the matrix element of interaction between these configurations and E_n is the configuration energy in the harmonic limit (i.e., the QRPA energy for $n = 1$, etc.). In the hierarchy of complex configurations the most important couplings are the ones with $\Delta n = n' - n = \pm 1$ because on average $V_{n\pm1}^n$ is about two–three orders of magnitude larger than $V_{n\pm2}^n$, etc. Since the most of physical observables are determined by 1ph configurations, the

QPM provides their description on a good level even without accounting for very complex configurations like in the IBM.

In actual calculations the model space of the qp $\otimes$ $n$ph configurations has been truncated at 6.5, 7.5, and 8.5 MeV for $n = 1, 2, 3$, respectively. The total number of configurations is about 1000 for each j^π. Concerning the truncation of the model space in comparison to the IBM, the QPM basis does not include configurations more complex than the qp $\otimes$ 3ph ones which are located above 2 MeV.

3.3. The ^{113}Cd nucleus

We present below a comparison of these calculations with the known experimental data. Figs. 5 and 6 show a comparison of the experimental and calculated level energies. For some of the levels, generally the first two of each spin, a correspondence with calculated levels is indicated. These correspondences have been made not only on the basis of level energies, but also taking into account other properties, such as electromagnetic decay branching ratios and spectroscopic factors. Occasionally, other known quantities like static electromagnetic moments and mixing ratios have been compared, when known [7]. The branching ratios calculated with the IBFM-1 are compared to the experimental ones in Table 3. The level schemes calculated with both the IBFM-1 and QPM for the positive parity (Fig. 5) resemble rather well the experimental one up to about 2 MeV, both with respect to the number of levels and their distribution in energy. Some more obvious exceptions will be discussed below. In Fig. 6 one can see that in the case of the negative parity

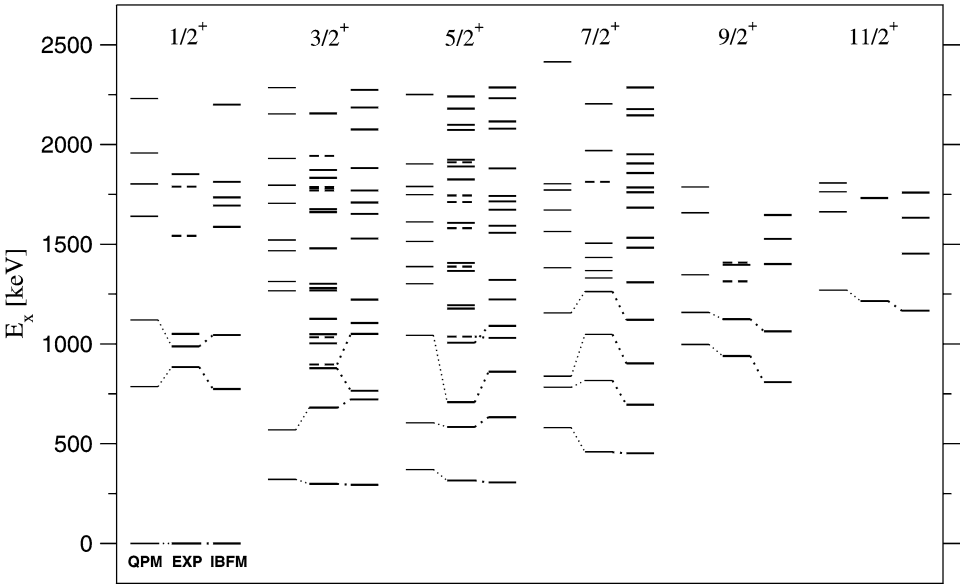

Fig. 5. Comparison between experimental levels and those calculated with the IBFM-1, for positive parity. Experimental levels with only tentative spin assignment (Table 2) are drawn with dashed lines. Dotted lines indicate assignments of the experimental levels to the calculated ones, see the discussion in text.

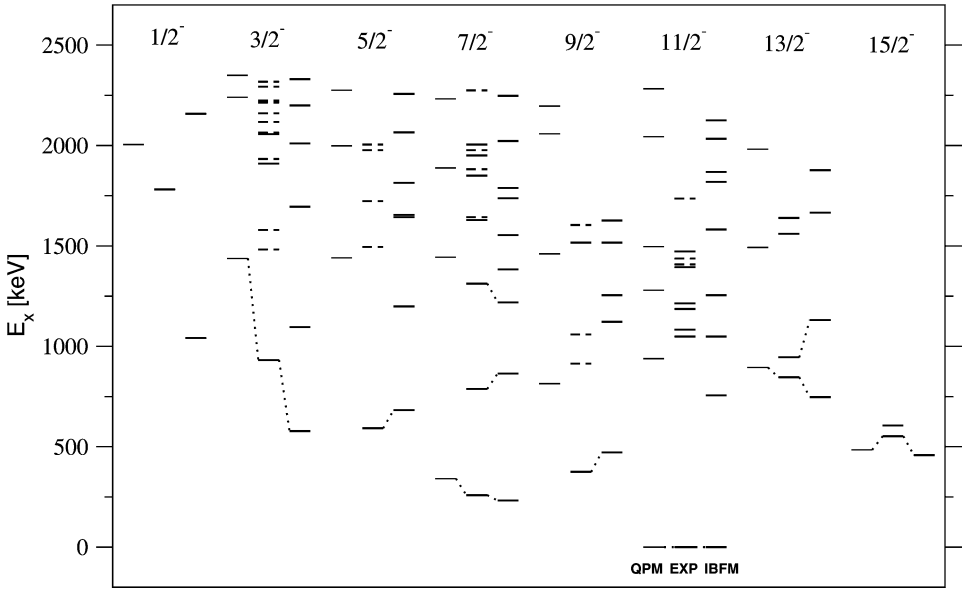

Fig. 6. Same as Fig. 5, but for negative parity levels. The energies are given relative to that of the first $11/2^-$ level.

levels the IBFM gives a reasonable description of the lowest levels of each spin. Surprisingly, the number of levels predicted by the QPM up to about 2.3 MeV excitation is too low compared to both experiment and the IBFM.

The QPM problems with the level density at low excitation energy are caused by a very strong anharmonicity of the 2_1^+ state in ^{112}Cd core. The energy of the first 2^+ phonon in this nucleus is about 1 MeV higher in the QRPA calculation compared to the experimental energy of the 2_1^+ level. The interaction with complex configurations shifts the lowest 2^+ state to its experimental value. In the case of such a strong anharmonicity, not only $(n \pm 1)$ph but also $(n \pm 2)$ph configurations begin to play an important role in the correct description of the states which carry the main part of the strength of an $n$ph configuration. Indeed, the energy of the $(n \pm 1)$ph configurations enter the denominator of Eq. (1) and for a good description of its value $(n \pm 2)$ph configurations are needed. In other words, Eq. (1) for estimation of the energy shift of an $n$ph configuration is transformed into a more complex one:

$$\Delta E_n \approx \frac{[V^n_{n\pm1}]^2}{E_n - (E_{n\pm1} - \frac{[V^{n\pm1}_{n\pm2}]^2}{E_{n\pm1-\cdots}})}. \tag{2}$$

As already pointed out, the unpaired neutron in the ground state of ^{113}Cd is located in the middle of $N = 50$–82 shell. Accordingly, the neutron quasiparticle levels closest to the Fermi surface are $1g_{7/2}$, $3s_{1/2}$, $2d_{3/2}$, $1h_{11/2}$, and $2d_{5/2}$. The above levels are listed in the order of their excitation energies in the employed mean-field in the QPM calculations.

Table 3
Comparison of experimental [7] and IBFM-calculated branching ratios of electromagnetic decays in ^{113}Cd

E_x	J_i	J_f	E_γ	Exp.	IBFM
0.3162	$5/2^+_1$	$1/2^+_1$	0.3162	100(4)	100.0
		$3/2^+_1$	0.0176	3.1(4)	74.0
0.4586	$7/2^+_1$	$5/2^+_1$	0.1424	100.0	100.0
0.5840	$5/2^+_2$	$1/2^+_1$	0.5840	100(1)	100.0
		$3/2^+_1$	0.2854	1.4(2)	2.9
		$5/2^+_1$	0.2678	2.5(2)	8.7
		$7/2^+_1$	0.1254	< 10	0.3
0.6806	$3/2^+_2$	$1/2^+_1$	0.6806	100(2)	100.0
		$3/2^+_1$	0.3820	20.9(4)	15.7
		$5/2^+_1$	0.3644	20.1(4)	1.1
		$5/2^+_2$	0.0966	5.3(3)	1.1
0.7086	$5/2^+_3$	$1/2^+_1$	0.7086	100(2)	10.5
		$3/2^+_1$	0.4100	11(2)	100.0
		$5/2^+_1$	0.3924	100(2)	5.7
		$7/2^+_1$	0.2500	11(1)	7.7
0.8167	$7/2^+_2$	$5/2^+_1$	0.5005	100(2)	100.0
		$7/2^+_1$	0.3581	35(1)	23.3
		$5/2^+_2$	0.2327	–	7.1
		$3/2^+_1$	0.5181	3.2(2)	0.4
0.8784	$3/2^+_3$	$1/2^+_1$	0.8784	100(15)	86.0
		$3/2^+_1$	0.5798	–	18.3
		$5/2^+_2$	0.5622	100(15)	100.0
		$7/2^+_1$	0.4198	9.2(23)	0.2
		$5/2^+_1$	0.2944	48(14)	33.0
0.8836	$1/2^+_2$	$1/2^+_1$	0.8836	100(2)	100.0
		$3/2^+_1$	0.5850	3.5(18)	7.0
0.8975	$3/2^+_4$	$1/2^+_1$	0.8975	–	8.8
		$3/2^+_1$	0.5989	100(2)	10.2
		$5/2^+_1$	0.5813	9(4)	100.0
		$7/1^+_1$	0.4389	22.4(7)	0.0
		$5/2^+_2$	0.3135	12.4(4)	17.2
0.9398	$9/2^+_1$	$5/2^+_1$	0.6236	51(2)	32.1
		$7/2^+_1$	0.4812	100(2)	100.0
0.9883	$1/2^+_3$	$1/2^+_1$	0.9883	100(8)	8.9
		$3/2^+_1$	0.6897	–	100.0
		$5/2^+_1$	0.6721	–	48.7
		$5/2^+_2$	0.4043	2.5(4)	12.3
		$5/2^+_3$	0.2797	2.5(4)	0.1

Table 3 (*continued*)

E_x	J_i	J_f	E_γ	Exp.	IBFM
1.0075	$5/2^+_5$	$1/2^+_1$	1.0075	–	7.0
		$3/2^+_1$	0.6913	100(15)	58.3
		$5/2^+_1$	0.5489	35(7)	100.0
		$7/1^+_1$	0.4235	6.5(12)	20.4
		$7/2^+_2$	0.1908	–	40.2
1.0374	$5/2^+_4$	$1/2^+_1$	1.0374	55(5)	2.2
		$3/2^+_1$	0.7388	88(24)	100.0
		$5/2^+_1$	0.7212	100(28)	24.4
		$7/1^+_1$	0.5788	–	4.9
		$5/2^+_2$	0.4534	14(3)	21.4
		$3/2^+_2$	0.3568	9(3)	8.0
1.0480	$7/2^+_3$	$3/2^+_1$	0.7494	–	100.0
		$5/2^+_1$	0.7318	100(4)	5.8
		$7/2^+_1$	0.5894	42(2)	3.4
		$5/1^+_2$	0.4640	16(2)	5.5
		$7/2^+_2$	0.2313	2.2(9)	3.6
1.1250	$9/2^+_2$	$5/2^+_1$	0.8088	41(3)	100.0
		$7/2^+_1$	0.6664	100(3)	5.0
		$5/2^+_3$	0.4164	24(1)	0.2
		$7/1^+_2$	0.3083	19(1)	32.3
		$9/2^+_1$	0.1852	6.3(8)	3.2
1.2147	$11/2^+_1$	$7/2^+_1$	0.7561	100(3)	100.0
		$9/2^+_1$	0.2749	7(4)	4.1
1.2620	$7/2^+_4$	$3/2^+_1$	0.9634	–	6.6
		$5/2^+_1$	0.9458	67(33)	14.3
		$7/2^+_1$	0.8034	100(11)	100.0
		$5/2^+_2$	0.6780	79(10)	19.9
		$3/2^+_2$	0.5814	–	6.9
		$5/2^+_3$	0.5534	–	67.3
		$7/2^+_2$	0.4453	38(8)	1.0
0.6382	$9/2^-_1$	$11/2^-_1$	0.3747	100	100.0
		$7/2^-_1$	0.1159	12.5(1.9)	12.5
0.8153	$15/2^-_1$	$11/2^-_1$	0.5518	100	100.0
0.8553	$5/2^-_1$	$7/2^-_1$	0.3330	100(2)	100.0
		$9/2^-_1$	0.2171	4.7(3)	3.7
0.8698	$15/2^-_2$	$11/2^-_1$	0.6063	100	33.2
		$15/2^-_1$	0.0545	–	100.0
1.0512	$7/2^-_2$	$7/2^-_1$	0.5289	49(2)	45.0
		$9/2^-_1$	0.4130	100(2)	100.0
		$5/2^-_1$	0.1959	–	83.2

(*continued on next page*)

Table 3 (*continued*)

E_x	J_i	J_f	E_γ	Exp.	IBFM
1.1093	$13/2^-_1$	$11/2^-_1$	0.8458	100(2)	100.0
		$9/2^-_1$	0.4711	4.3(7)	3.9
		$15/2^-_1$	0.2940	24.0(8)	10.2
		$15/2^-_2$	0.2395	–	1.8
1.1777	$7/2^-_3$	$7/2^-_1$	0.6554	100(4)	100.0
		$9/2^-_1$	0.5395	–	83.4
		$5/2^-_1$	0.3224	60.8(23)	19.6
		$7/2^-_2$	0.1265	33(3)	0.0
1.1946	$3/2^-_1$	$7/2^-_1$	0.6723	100(6)	68.7
		$5/2^-_1$	0.3393	99(5)	100.0
1.2095	$13/2^-_2$	$11/2^-_1$	0.9460	100	100.0
		$9/2^-_1$	0.5713	–	35.6
		$15/2^-_1$	0.3942	–	24.0
		$15/2^-_2$	0.3397	–	71.7
1.3465	$11/2^-_2$	$11/2^-_1$	1.0830	–	65.6
		$7/2^-_1$	0.8242	100	36.7
		$9/2^-_1$	0.7083	–	100.0
		$15/2^-_2$	0.4767	–	5.6
1.7460	$3/2^-_2$	$5/2^-_1$	0.8907	100	100.0
		$7/2^-_2$	0.6948	–	5.9
		$3/2^-_1$	0.5514	–	9.8

The experimental levels with excitation energy given in the first column have been assigned to the calculated levels with J^π indicated in the second column. Calculated values smaller than 5% are given only if there is a measured value.

We denote these levels as j_{Fs}. The energy difference between the quasiparticle energies of $1g_{7/2}$ and $2d_{5/2}$ levels is only 450 keV.

An interaction with complex configurations which is different for different j^π, makes the $1/2^+_1$ state the lowest in energy (the ground state) and the isomeric state $11/2^-_1$ as the first excited state in agreement with the data. The order of the next excited states $3/2^+_1$, $5/2^+_1$, and $7/2^+_1$ and the absolute values of their excitation energies is also well reproduced in calculations. The main component of the wave functions of these states is the quasiparticle configuration with the corresponding j^π quantum numbers. Its contribution varies from 83% for the $1/2^+_1$ state to 72% for the $5/2^+_1$ state.

About 600 keV higher in energy the states which carry a big fraction of $[j_{Fs} \otimes 2^+_1]_{j^\pi}$ configurations are located. Since there is only one configuration of this type for $j^\pi = 11/2^+$ and for the states with negative parity, the corresponding configuration is rather pure in the wave function of the $11/2^+_1$, $11/2^-_2$, $7/2^-_1$, $9/2^-_1$, $13/2^-_1$, and $15/2^-_1$ states. For other states with positive parity, the $[j_{Fs} \otimes 2^+_1]_{j^\pi}$ configurations are strongly mixed in the wave functions of the $1/2^+_{2,3,4}$, $3/2^+_{2,3,4,5}$, $5/2^+_{2,3,4,5}$, $7/2^+_{2,3,4}$, and $9/2^+_{1,2}$ states. As far as

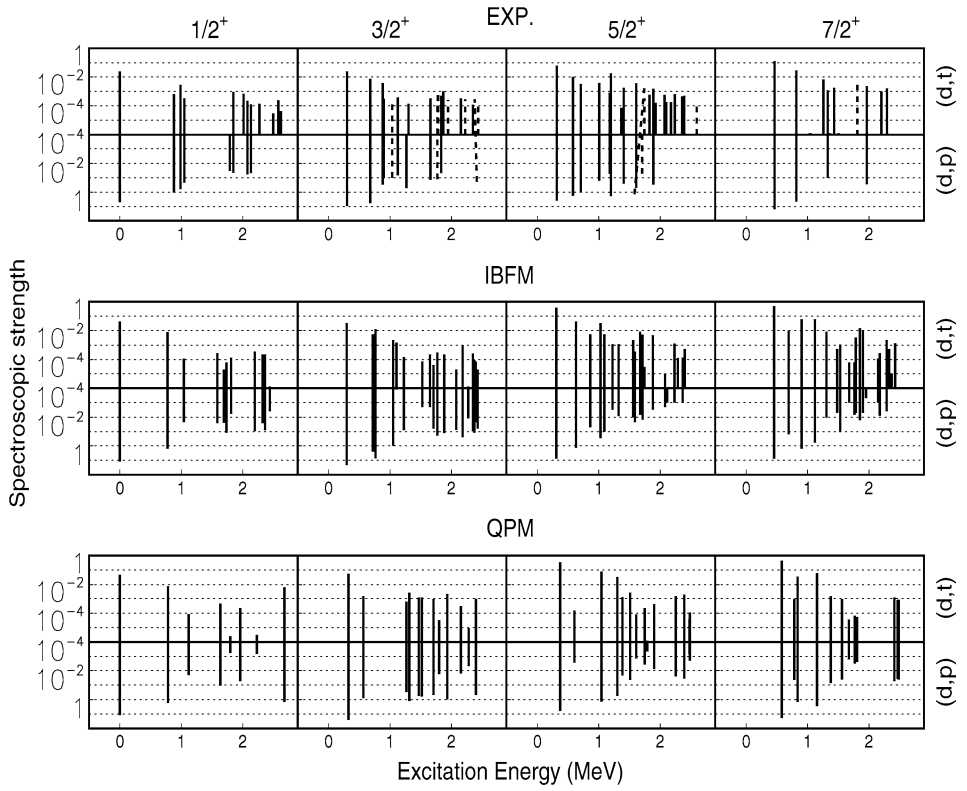

Fig. 7. Experimental and calculated (IBFM-1) spectroscopic strengths for positive parity states in ^{113}Cd populated by the pickup and stripping of one neutron. All observed and calculated states up to 2.6 MeV excitation are represented.

the QPM model space includes up to qp ⊗ 3ph configurations, the experimental values of their excitation energies are described rather well in the calculation.

The next in energy appear the states with configurations $[j_{Fs} \otimes [2_1^+ \otimes 2_1^+]_{0^+,2^+,4^+}]$. As it is clear from the above discussion, qp ⊗ 4ph configurations should play an important role in the correct description of the energies of these states. Unfortunately, we are not able to include such complex configurations in the QPM model space for technical reasons. That is why the energies of these states are over-predicted in the QPM calculation while they are described rather well in the IBM calculation. With only one negative parity quasiparticle level among j_{Fs}, the number of j^- states is very low in the QPM calculation below 2.5 MeV. The states with $[j_{Fs}^+ \otimes 3_1^-]_{j_{Fs}^-}$ configurations involving the 3_1^- phonon to change the parity, are located between 2.0 and 2.5 MeV and the configurations including non-collective positive parity phonons are located above 2.5 MeV.

Fig. 7 shows the distribution in energy of the positive parity levels and of their spectroscopic strengths; the experimental and calculated (by both models) fragmentations of the four shells show a good similarity. A more quantitative comparison for the summed spectroscopic strengths is made in Table 4 and Fig. 8. In both model calculations, these

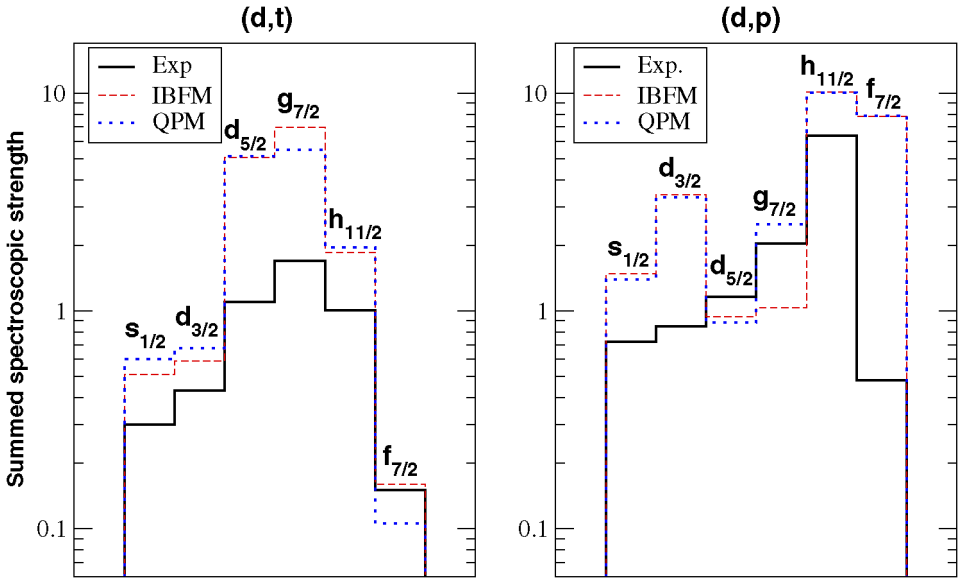

Fig. 8. Experimental (full lines) and theoretical (dashed lines) integrated one-neutron transfer strengths. See Table 4 for numerical values and the text for details.

Table 4
Sum rules for spectroscopic strengths

Shell	Reaction					
	(d,t)			(d,p)		
	Exp.	IBFM	QPM	Exp.	IBFM	QPM
$3s_{1/2}$	0.30	0.51	0.60	0.72	1.49	1.40
$2d_{3/2}$	0.43	0.59	0.68	0.85	3.41	3.32
$2d_{5/2}$	1.10	5.06	5.12	1.16	0.94	0.88
$1g_{7/2}$	1.70	6.97	5.50	2.04	1.03	2.49
$1h_{11/2}$	1.01	1.86	1.96	6.38	10.14	10.04
$1h_{9/2}$	0.02	0.08	0.06	0.11	9.92	9.94
$2f_{7/2}$	0.15	0.16	0.11	0.48	7.84	7.89
$2f_{5/2}$	–	–	0.04	–	–	5.96
$3p_{3/2}$	0.001	0.04	0.04	0.17	3.96	3.96
$3p_{1/2}$	0.009	0.02	–	0.03	1.98	–

The experimentally observed (up to 2.6 MeV excitation) integrated strengths for the two reactions are compared with the sum rule limits given by the BCS v_j^2 values used in the IBFM-1 and QPM calculations, respectively.

sum rules are given by the shell occupancies derived from a BCS calculation on the chosen single particle level scheme. Then, for the sum of the spectroscopic factors S_{lj} of all states of the same spin j assigned to a certain orbital (ℓ, j) we get simply v_j^2 and $(1 - v_j^2)$ for the pickup and stripping of a neutron, respectively; for the summed spectroscopic strengths $G_{lj} = (2j + 1)S_{lj}$, one gets the number of particles (holes) in that orbital. From Fig. 8 and Table 4, one can see that the experimental strength for the $3s_{1/2}$ and $2d_{3/2}$ shells is

below the theoretical expectation; thus, it appears that not all the states have been observed up to 2.5 MeV. For the $2d_{5/2}$ and $1g_{7/2}$ shells, it appears that one has not observed the whole predicted pickup strength, but one has practically exhausted the stripping strength. The overall agreement (Figs. 5 to 8, Tables 3 and 4) is reasonable for most of the low-lying levels, and this will allow a qualitative discussion of their structure. The sum rule limits given by the QPM calculations are rather similar with those given by the IBFM-1; a slight improvement occurs for the $g_{7/2}$ shell.

For the negative parity orbitals, one can state the following. We have observed a large fraction of the expected $h_{11/2}$ strength, both in pickup and in stripping (Table 4, Fig. 8). For the $2f_{7/2}$ shell, we have excited in (d,t) five states up to 2.27 MeV, and they contain practically the whole expected pickup strength—actually, in the IBFM approach this is due to our adjustment of the single particle energy of this orbital, as stated in Section 3.1, such as to get for it $v_j^2 = 0.02$. No state with $J^\pi = 5/2^-$ was populated in our reactions. As concerns the $3p_{1/2}$ and $3p_{3/2}$ shells, only one $1/2^-$ state has been observed, but a large number of $3/2^-$ states have been seen up to the highest energies reached in this study; they represent only the tail of the fragmentation distributions of these shells which are expected at higher excitation energies.

3.3.1. Structure of the positive parity states

Table 5 presents the composition of the wavefunctions of some of the IBFM-1 calculated states. In Fig. 9 we have classified the lowest calculated levels according to their dominant component in the wavefunction. This classification corresponds, as seen in this figure, to the multiplets resulting from coupling the four (ℓ, j) positive parity quasiparticles to the 0_1^+ and 2_1^+ states of the core. The classification is only approximate, since some of the wavefunction are rather mixed, but the multiplets are complete, practically all the expected states could be identified. A slight exception is the $1/2^+$ state of the $2_1^+ \otimes d_{3/2}$ multiplet. The calculated $1/2_3^+$ state, although with only a small $d_{3/2}$ component, has been placed within this multiplet since it falls about in the right position. The next step has been the identification of the experimental levels which correspond to these multiplets, by checking the properties of these levels, and especially their electromagnetic decays (branching ratios, Table 3). For most of the levels the comparison of the branching ratios allowed a rather unambiguous assignment to one of the calculated levels; a somewhat weaker agreement has been obtained for the levels assigned to the $3/2_4^+$, $5/2_3^+$ and $7/2_3^+$ calculated states—in these cases, although the strongest branch was not correctly predicted, still there is an agreement concerning the branches which are important in the decay of those states. The experimental counterpart of the theoretical $3/2_5^+$ state could not be assigned with certainty, but there are two candidates in the right position (the states at 1034 and 1258 keV—drawn in the right side of Fig. 9). The $1/2_3^+$ state has been only tentatively associated with the state at 988 keV, since its electromagnetic decay is not reproduced, and that of the other $1/2^+$ state at 1050 keV is not known. Trying to decide on the basis of the spectroscopic factors is also ambiguous, since one compares the calculated spectroscopic strengths of the $1/2_3^+$ state for the $(d,t)/(d,p)$ reaction of 0.007/0.035, with the experimental values 0.028/0.064 and 0.0033/0.022 for the 988 and 1050 keV states, respectively. Fig. 9 contains practically all experimental and calculated (IBFM-1) positive parity levels up to about 1.25 MeV. There is an obvious excess of experimental $1/2^+$ and $3/2^+$ levels in the

Table 5
Wavefunction composition for some of the IBFM-1 calculated levels

Positive parity					
J^π	E_x (MeV)	$s_{1/2}$ (%)	$d_{3/2}$ (%)	$d_{5/2}$ (%)	$g_{7/2}$ (%)
$1/2_1^+$	0.000	86.6	8.1	4.6	0.6
$1/2_2^+$	0.775	14.5	28.6	54.8	1.8
$1/2_3^+$	1.044	37.4	9.3	30.7	22.5
$1/2_4^+$	1.586	12.1	22.9	33.1	31.8
$1/2_5^+$	1.694	4.3	5.6	62.5	27.4
$3/2_1^+$	0.294	18.4	70.6	3.5	7.3
$3/2_2^+$	0.722	4.7	9.0	81.8	4.4
$3/2_3^+$	0.766	38.7	27.1	10.7	23.3
$3/2_4^+$	1.051	29.3	50.8	9.4	10.3
$3/2_5^+$	1.105	10.5	20.0	22.1	47.3
$3/2_6^+$	1.222	0.0	2.5	81.2	16.2
$5/2_1^+$	0.306	1.6	0.5	96.1	1.6
$5/2_2^+$	0.633	65.4	8.0	24.6	1.8
$5/2_3^+$	0.862	1.8	2.1	32.2	63.7
$5/2_4^+$	1.031	18.4	5.1	46.5	29.8
$5/2_5^+$	1.091	13.1	74.7	5.4	6.5
$5/2_6^+$	1.223	3.4	7.3	75.9	13.2
$7/2_1^+$	0.452	0.0	2.3	5.0	92.5
$7/2_2^+$	0.696	0.2	0.8	88.3	10.4
$7/2_3^+$	0.903	3.8	50.8	5.9	29.3
$7/2_4^+$	1.122	4.4	9.3	26.8	59.4
$7/2_5^+$	1.309	1.3	18.6	22.4	57.5
$7/2_6^+$	1.482	4.2	2.1	42.3	51.1
$9/2_1^+$	0.809	0.3	0.5	13.3	85.8
$9/2_2^+$	1.064	0.6	1.9	69.2	18.2
$9/2_3^+$	1.401	0.0	6.0	37.8	6.0
$11/2_1^+$	1.167	0.2	7.1	19.2	73.3

Negative parity						
J^π	E_x (MeV)	$h_{11/2}$ (%)	$f_{7/2}$ (%)	$p_{3/2}$ (%)	$h_{9/2}$ (%)	$p_{1/2}$ (%)
$1/2_1^-$	2.045	92.3	7.3	0.28	0.01	0.0050
$3/2_1^-$	1.195	93.0	6.7	0.16	0.02	0.0020
$5/2_1^-$	0.855	94.5	5.3	0.06	0.06	0.0003
$7/2_1^-$	0.522	94.6	5.2	0.07	0.03	0.0007
$9/2_1^-$	0.638	96.9	2.9	0.02	0.06	0.0001
$11/2_1^-$	0.264	97.2	2.7	0.03	0.02	0.0002
$13/2_1^-$	1.109	97.4	2.4	0.02	0.06	0.0001
$15/2_1^-$	0.815	95.5	4.3	0.07	0.03	0.0005

The second column gives the calculated excitation energy (in the case of the negative parity states, the values were normalized to the experimental value of the $11/2_1^-$ state).

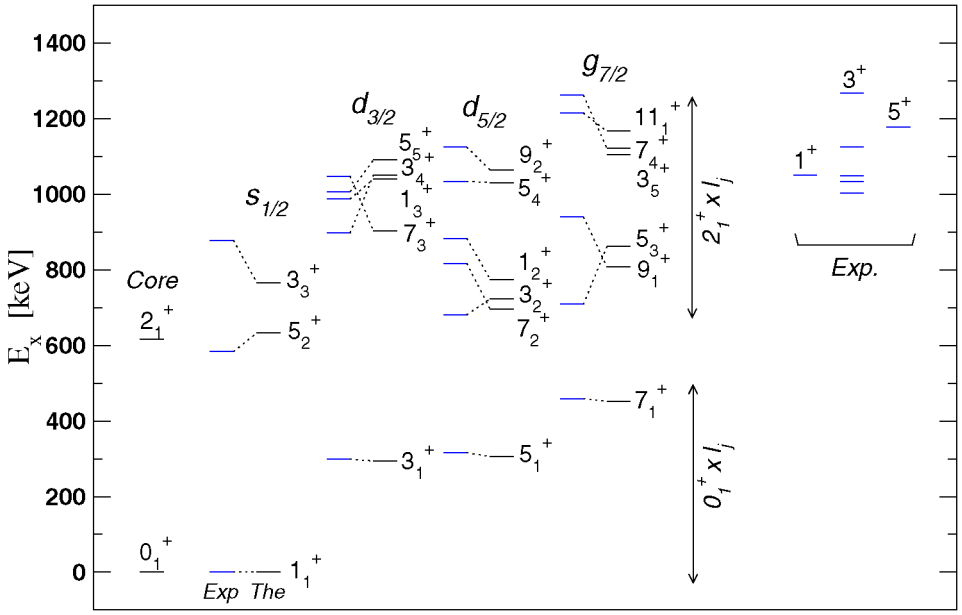

Fig. 9. Positive parity multiplet structures in the low excitation energy part of ^{113}Cd. The theoretical levels were calculated with the IBFM-1 and have been classified as shown according to the dominant quasiparticle component in the wavefunction (Table 5). The levels are labeled with the double of the spin value and their order number. The experimental levels were put into correspondence with the theoretical ones on the basis of their properties. Possible intruder levels, resulting by coupling of the $s_{1/2}$ and $d_{3/2}$ quasiparticle orbitals to the low-lying intruder 0^+ state in ^{112}Cd, are among the levels shown in the right part of the figure. See text for more detailed comments of this figure.

1.0–1.2 MeV region. Thus, one can propose that one of the two $1/2^+$ levels at 988 and 1050 keV is an *intruder* state, that is, having as main structure that of an $s_{1/2}$ quasiparticle coupled to the intruder 0^+, 1224 keV state of the core. Qualitatively, on the basis of the (d, t) spectroscopic factors, a better candidate seems to be the 1050 keV state (as proposed also in [5]) since for a state which has only a small component of the 0^+ ground state of the core in the wavefunction one expects a smaller spectroscopic factor. Similarly, we have one or two additional $3/2^+$ states in the same energy region (among the states at 1003, 1034, 1049, 1126 keV), which have no theoretical counterpart, therefore they could be also intruders of $d_{3/2}$ origin. Note that in the language above, "intruder" refers to 2p–2h states of the core, which do not belong to the IBM space. In the case of the QPM calculations, as it results from the discussion above, the energy of such states should be overestimated.

3.3.2. Structure of the negative parity states

The wavefunction composition of some of the negative parity states calculated with the IBFM-1 is also given in Table 5. They are all dominated by the $1h_{11/2}$ orbital. The next important orbital is $2f_{7/2}$ which has larger contribution (up to 7%) in the low spin states, and less (below 3%) in the higher spin states. Table 3 shows that the decay of the lower

negative parity states is reasonably well reproduced. Note that the branching ratios of the lowest two $3/2^-$ ('antialigned') states are also well described.

A relatively large number of $\ell = 1$ states (some of them firmly assigned as $3/2^-$) have been confirmed or observed for the first time (especially in the (d, p) reaction) at higher excitation energies. The first three such states at 1195, 1746 and 1843 keV have not been observed in our reactions, while above 2 MeV nine states have been observed at the energies of 2174, 2320, 2327, 2381, 2424, 2477, 2488, 2556, 2591 keV (probably the same with the 2588 keV observed in [4] and assigned as $3/2^-$)—see Table 2. Thus, the distribution of the fragmentation of the $3p_{3/2}$ orbital is rather similar with that observed in the Te isotopes 123, 125, and 129, with the (d, p) and (n, γ) reactions [6]. In ^{113}Cd, we know the γ-ray decay only for the lowest two $3/2^-$ states: they preferentially decay to the $5/2^-_1$ state. For the higher states (above 2 MeV) the gamma decay is not known, but the similarity with the Tellurium isotopes is so good that one may assume that their structure is similar too, in such a way that these states also decay preferentially towards the same $5/2^-_1$ state. The $5/2^-_1$ states decays mainly to the $7/2^-_1$ state, which, in turn, decays mainly to the $11/2^-_1$ isomer. Therefore, the observed $3/2^-$ states very probably play the role of "gateway" in the (γ, γ') process, and thus, through their decay to the $5/2^-_1$ "funnel" state, one can obtain a strong population of the $11/2^-$ isomeric state [6].

4. Conclusions

The present work reported a detailed study of the structure of ^{113}Cd, by means of high resolution one-neutron transfer reaction experiments (d, p) and (d, t) with a polarized deuteron beam. Up to 2.6 excitation energy a number of about 80 levels have been observed in both reactions, and spin and parities and spectroscopic factors have been determined for many of them.

A detailed comparison of the experimental data is made with prediction of two theoretical models: the interacting boson–fermion model-1 (IBFM-1) and the quadrupole phonon model (QPM). The lowest excitation energy part of the spectrum, up to about 1.3 MeV, is well understood, as representing mainly the multiplets resulting from the coupling of the quasiparticle orbitals of the 50–82 shell to the 2^+ quadrupole vibration of the core. The states above this energy, up to about 2.5 MeV excitation have more complex (mixed) structures, and cannot be put into one-to-one correspondence with the experimental ones. Nevertheless, the distribution functions of the transfer strengths for the different orbitals are generally well reproduced by the model calculations. The QPM calculations are found to overestimate the excitation energies of some states, especially those with negative parity. This effect is the result of a strong anharmonicity of the 2^+_1 state in the ^{112}Cd core, and shows the need to take into account a large number of more complex configurations, which could not be done for technical reasons.

Many $(3/2^-)$ states have been observed in the excitation region 2.1–2.6 MeV, and it is suggested, by similarity with the Tellurium isotopes, that they play an important role in the population of the $11/2^-$ isomeric state through the (γ, γ') reaction.

Note added in proof

The tabulated experimental data are available as entry No. D0310 in the EXFOR database of the IAEA (http://www-nds.iaea.ro).

Acknowledgements

We thank Drs. D. Hofer and Zs. Nemeth for their contribution in the early phases of this project. D.B. acknowledges support within a Deutsche Forschungsgemeinschaft Grant (II C4-Gr894/1-3) during working stages at the Ludwig Maximilians Universität in München, and V.Yu.P. acknowledges support by the Deutsche Forschungsgemeinschaft (SFB 634). This work was partly founded within a CERES project of the Romanian Ministery for Education and Research.

References

[1] D. De Frenne, E. Jacobs, Nucl. Data Sheets 79 (1996) 639.
[2] J. Blachot, Nucl. Data Sheets 75 (1995) 739.
[3] P.E. Garrett, H. Lehmann, J. Jolie, C.A. McGrath, in: J. Kvasil, P. Cejnar, M. Krtiča (Eds.), Proceedings of the 11th International Symposium "Capture Gamma-Ray Spectroscopy and Related Topics", Prague, 2002, World Scientific, Singapore, 2003, p. 157.
[4] W. Geiger, et al., Nucl. Phys. A 580 (1994) 263.
[5] N. Warr, et al., Nucl. Phys. A 620 (1997) 127.
[6] V. Bondarenko, et al., Phys. Rev. C 60 (1999) 027302.
[7] J. Blachot, Nucl. Data Sheets 83 (1998) 647.
[8] Zs. Nemeth, et al., in: J. Kern (Ed.), Proceedings of the 8th International Symposium "Capture Gamma-Ray Spectroscopy and Related Topics", Fribour, 1993, World Scientific, Singapore, 1994, p. 314.
[9] Z.I. Matumoto, T. Tamura, K. Sakuray, J. Phys. Soc. Jpn. 44 (1978) 1062;
B. Fogelberg, et al., Z. Phys. A 337 (1990) 251.
[10] M. Hoike, Nucl. Phys. A 98 (1967) 209.
[11] R.K. Jolly, E.K. Lin, B.L. Cohen, Phys. Rev. 128 (1962) 2292.
[12] L.H. Goldman, J. Kremenek, S. Hinds, Phys. Rev. 179 (1969) 1172.
[13] N. Fotiades, et al., Phys. Rev. C 61 (2000) 064326;
N. Buforn, et al., Phys. Scr. 88 (2000) 45.
[14] P. Schiemenz, F.J. Eckle, G. Eckle, G. Graw, H. Kader, F. Merz, in: M. Kondo, et al. (Eds.), Proceedings of the Sixth International Symposium on Polarization Phenomena in Nuclear Physics, Physical Society of Japan, Tokyo, 1985, p. 1056.
[15] M. Löffler, H.J. Scheerer, H. Vonach, Nucl. Instrum. Methods 111 (1973) 1.
[16] E. Zanotti, M. Bisenberger, R. Hertenberger, H. Kader, G. Graw, Nucl. Instrum. Methods A 310 (1991) 706.
[17] D. Bucurescu, et al., Nucl. Phys. A 672 (2000) 21.
[18] J.K. Tuli, Nucl. Data Sheets 86 (1999) 285.
[19] P.D. Kunz, Computer code CHUCK3, University of Colorado, unpublished.
[20] C.M. Perey, F.G. Perey, At. Data Nucl. Data Tables 17 (1976) 1;
W.W. Daehnick, J.D. Childs, Z. Vrcelj, Phys. Rev. 221 (1980) 2253.
[21] F. Iachello, O. Scholten, Phys. Rev. Lett. 43 (1979) 679.
[22] F. Iachello, A. Arima, The Interacting Boson Model, Cambridge Univ. Press, Cambridge, MA, 1987.
[23] O. Scholten, Computer codes PHINT and FBEM, KVI Report No. 63, unpublished.
[24] P.O. Lipas, E. Hammaren, P. Toivonen, Phys. Lett. B 139 (1984) 10.

[25] M. Délèze, et al., Nucl. Phys. A 554 (1993) 1.
[26] R. Hertenberger, et al., Nucl. Phys. A 574 (1994) 414.
[27] O. Scholten, Computer codes ODDA and PBEM, KVI Internal report No. 252 (1982); computer code SPEC, unpublished.
[28] T.T.S. Kuo, E. Baranger, M. Baranger, Nucl. Phys. 81 (1966) 4241.
[29] W. Nazarewicz, J. Dudek, R. Bengtsson, T. Bengtsson, I. Ragnarsson, Nucl. Phys. A 345 (1985) 397.
[30] R. Bijker, A.E.L. Dieperink, Nucl. Phys. A 379 (1982) 221;
R. Bijker, O. Scholten, Phys. Rev. C 32 (1985) 591.
[31] W.-T. Chou, N.V. Zamfir, R.F. Casten, Phys. Rev. C 56 (1997) 829.
[32] O. Scholten, T. Ozzello, Nucl. Phys. A 424 (1984) 221.
[33] V.G. Soloviev, Theory of Atomic Nuclei: Quasiparticles and Phonons, Institute of Physics, Bristol and Philadelphia, 1992.
[34] A.I. Vdovin, V.V. Voronov, V.G. Soloviev, Ch. Stoyanov, Part. Nucl. 16 (1985) 245.
[35] V.Yu. Ponomarev, A.P. Dubensky, V.P. Dubensky, E.A. Boykova, J. Phys. G 16 (1990) 1727.
[36] J.J. Caroll, C.J. Collins, K. Heyde, M. Huber, P. von Neumann-Cosel, V.Tu. Ponomarev, D.G. Richmond, A. Richter, C. Schlegel, T.W. Sinor, K.N. Taylor, Phys. Rev. C 48 (1993) 2238.
[37] H.-F. Wirth, T. von Egidy, I. Tomandl, J. Honzátko, D. Bucurescu, N. Mărginean, V.Yu. Ponomarev, R. Hertenberger, Y. Eisermann, G. Graw, Nucl. Phys. A 716 (2003) 3.
[38] I. Tomandl, T. von Egidy, J. Honzátko, V. Bondarenko, H.-F. Wirth, D. Bucurescu, V.Yu. Ponomarev, G. Graw, R. Hertenberger, Y. Eisermann, S. Raman, Nucl. Phys. A 717 (2003) 149.
[39] K. Takeuchi, P.A. Moldauer, Phys. Lett. B 28 (1969) 384.
[40] V.A. Chepurnov, Sov. J. Nucl. Phys. 16 (1967) 955.
[41] S. Gales, Ch. Stoyanov, A.I. Vdovin, Phys. Rep. 166 (1988) 125.
[42] J. Bryssinck, et al., Phys. Rev. C 62 (2000) 014309.